

Synthesis, Structure, and Properties of $A_{14}AlSb_{11}$ ($A = Ca, Sr, Ba$)

STEPHANIE L. BROCK, LAURA J. WESTON,
MARILYN M. OLMSTEAD, AND SUSAN M. KAUZLARICH*

Department of Chemistry, University of California, Davis, California 95616

Received February 5, 1993; in revised form April 19, 1993; accepted April 26, 1993

$A_{14}AlSb_{11}$ ($A = Ca, Sr, Ba$) is synthesized by reacting the elements in stoichiometric amounts at high temperature (1250°C). Single-crystal X-ray diffraction data (130 K: $a = 17.493$ (4) Å, $c = 23.480$ (8) Å (Sr); $a = 18.293$ (2) Å, $c = 24.222$ (9) Å (Ba)) were refined (tetragonal, $I4_1/acd$ (142), $Z = 8$; $R = 4.02\%$, $R_w = 4.26\%$ (Sr); $R = 3.71\%$, $R_w = 4.34\%$ (Ba)) and showed these compounds to be isostructural to $Ca_{14}AlSb_{11}$. Single-crystal X-ray and microprobe data indicate that these compounds are slightly deficient in Al. Temperature-dependent resistivity measurements show that these materials are intrinsic semiconductors with activation energies of 0.0143, 0.0667, and 0.4814 eV for the Ca, Sr, and Ba analogs, respectively. © 1993 Academic Press, Inc.

Introduction

There are number of ternary II–III–V compounds whose structures and bonding can be described according to the scheme of Zintl and others (1–5). Application of these bonding schemes to predict new transition metal compounds has been successful, and the compounds $A_{14}MnPn_{11}$ ($A = Ca, Sr, Ba$; $Pn = As, Sb, Bi$) have been synthesized (6–8). These compounds are isostructural to $Ca_{14}AlSb_{11}$ (9), the first compound synthesized with this structure type by Cordier *et al.* in 1984. The crystal structure was reported and an interpretation of the bonding, according to a modified Zintl concept, was given (9). The compound can be described as consisting of A^{2+} cations, Sb^{3-} anions, and covalently bonded tetrahedral $AlSb_4^{9-}$ and linear Sb_3^{7-} anions. This description of the structure type suggests that these compounds should exhibit semiconducting behavior. Electrical resistivity studies of the $A_{14}MnBi_{11}$ compounds show that these compounds are metallic (8, 10). Magnetic studies indicate, for all compounds measured to

date, that the Mn ions have four unpaired spins consistent with a Mn valence of +3 (6, 8, 10, 11). At temperatures less than 55 K, the $A_{14}MnPn_{11}$ ($Pn = Sb, Bi$) compounds order ferromagnetically with the exception of $Ba_{14}MnBi_{11}$ which orders antiferromagnetically (8, 10, 11). To further understand the unusual electronic and magnetic properties of the $A_{14}MnPn_{11}$ compounds we have investigated the main group analogs $A_{14}GaAs_{11}$ ($A = Ca, Sr$) and have proposed that these compounds are semiconducting based on their optical absorption (12, 13). In an effort to study the systematics in bonding as well as the electrical properties, we have synthesized the series of compounds, $A_{14}AlSb_{11}$ ($A = Ca, Sr, Ba$). We have obtained single-crystal X-ray diffraction data on the strontium and barium analogs and have obtained temperature-dependent resistivity on single crystals of $Ca_{14}AlSb_{11}$ and $Sr_{14}AlSb_{11}$ and on pressed powders of $Ca_{14}AlSb_{11}$ and $Ba_{14}AlSb_{11}$.

Experimental Section

Materials. The elements calcium (99.99%), and barium (99.9%) were obtained

* To whom correspondence should be addressed.

from Anderson Physics Labs. Strontium (99.95%) was obtained from Strem Chemicals. The alkaline earth elements and antimony (J. Matthey, 99.9999%) were used without further purification. Aluminum shot (Matheson, Coleman, and Boil, 99.6%) was cleaned with a 10% $\text{HNO}_3/\text{CH}_3\text{OH}$ solution and immediately transferred into the dry-box.

Synthesis. All of the $A_{14}\text{AlSb}_{11}$ ($A = \text{Ca}, \text{Sr}, \text{Ba}$) compounds were synthesized by mixing stoichiometric amounts of the appropriate elements. The reactants and products were handled in nitrogen-filled dry boxes with typical water levels less than 1 ppm. The reactants were placed into a Nb tube, which was arc welded closed under an atmosphere of Ar. The filled Nb tube was then sealed in a quartz ampoule under vacuum. The reaction vessel was placed in a furnace and heated to 600°C ($8^\circ/\text{min}$) followed by heating to 1250°C ($20^\circ/\text{hr}$). It was maintained at that temperature for 24 hr and first cooled to 600°C ($20^\circ/\text{hr}$) and then rapidly to room temperature ($8^\circ/\text{min}$). The resulting air-sensitive product was made up of a mixture of powder, chunks of a silver material, and a small amount of elongated diamond shaped or needle crystals. This mixture was essentially a quantitative yield of the desired product ($>90\%$ based on Guinier X-ray powder diffraction). In the case of the $\text{Sr}_{14}\text{AlSb}_{11}$, a reaction was also run using two times the stoichiometric amount of Al. There are no differences in the lattice parameters for the samples prepared stoichiometrically versus the one with excess Al.

Elemental analysis. Crystals of $\text{Ba}_{14}\text{AlSb}_{11}$, $\text{Sr}_{14}\text{AlSb}_{11}$, and $\text{Ca}_{14}\text{AlSb}_{11}$, embedded in indium, were examined using a Cameca SX50 electron microprobe with wavelength dispersive spectrometers. The microprobe was operated at 15 KeV accelerating potential and 10 nA beam current. The elemental analysis is based on 15 spots ($\text{Sr}_{14}\text{AlSb}_{11}$) or 12 spots ($\text{Ca}_{14}\text{AlSb}_{11}$) (spot size $1\ \mu\text{m}$) from two different crystals. The elemental analysis of $\text{Ba}_{14}\text{AlSb}_{11}$ is based on

15 spots on one crystal. During transfer to the microprobe, most of the $\text{Ba}_{14}\text{AlSb}_{11}$ crystals decomposed and reliable data (wt. concentration totals = 100%) were only obtained on one crystal. Decomposition was evident by the lack of smooth surfaces on the crystals in the reflected image. There was no evidence for any Nb in the crystals, which might have come from reaction with the container. Al, A ($A = \text{Ca}, \text{Sr}, \text{Ba}$), and Sb contents were determined using Al, ATiO_3 , and Freibergite ($\text{Cu}_7\text{Fe}_2\text{Ag}_3\text{Sb}_4\text{S}_{13}$) as standards, respectively. The result for $\text{Ba}_{14}\text{AlSb}_{11}$ is $\text{Ba}_{14.0(1)}\text{Al}_{1.12(4)}\text{Sb}_{10.9(1)}$. An accurate measure of Al cannot be obtained for this sample since the $\text{Ba } L\alpha_2$ line overlaps and is almost equal in intensity with the Al $K\alpha_1$ line. The results for crystals of $\text{Sr}_{14}\text{AlSb}_{11}$ are $\text{Sr}_{14.3(6)}\text{Al}_{0.8(1)}\text{Sb}_{10.9(5)}$ and $\text{Sr}_{14.2(4)}\text{Al}_{0.82(3)}\text{Sb}_{11.0(1)}$. The results for crystals of $\text{Ca}_{14}\text{AlSb}_{11}$ are $\text{Ca}_{14.0(2)}\text{Al}_{0.82(2)}\text{Sb}_{11.2(1)}$ and $\text{Ca}_{13.9(1)}\text{Al}_{0.84(3)}\text{Sb}_{11.3(1)}$.

X-ray powder diffraction. Characterization was carried out by X-ray powder techniques (Guinier) at room temperature. The sample was mounted between pieces of tape with NBS silicon included as an internal standard. The powder patterns were indexed according to information obtained from the single-crystal structural refinement. The corresponding lattice constants (see Table I) were determined by standard least-squares refinement. Lattice constants obtained for $\text{Ca}_{14}\text{AlSb}_{11}$ are $a = 16.672$ (6) Å and $c = 24.43$ (1) Å, in good agreement with the literature values (9). Room temperature lattice parameters for $A_{14}\text{AlSb}_{11}$ ($A = \text{Sr}, \text{Ba}$) are given in Table I.

Single-crystal X-ray study. The reaction container was opened in a dry box equipped with a microscope. Several crystals of $A_{14}\text{AlSb}_{11}$ ($A = \text{Sr}, \text{Ba}$) were coated with a hydrocarbon oil to minimize exposure to air. A suitable crystal ($0.08 \times 0.08 \times 0.32$ mm (Sr); $0.08 \times 0.08 \times 0.26$ mm (Ba)) was mounted on a glass fiber with silicone grease and positioned in a cold stream of nitrogen. The single crystal diffraction data were col-

TABLE I
 CRYSTALLOGRAPHIC PARAMETERS

Formula:	$Sr_{14}Al_{0.85}Sb_{11.15}$	$Ba_{14}Al_{0.96}Sb_{11.04}$
fw	2607.13	3292.78
Color and habit	black needle	black needle
Crystal system	Tetragonal	Tetragonal
Space group, Z	$I4_1/acd$, 8	$I4_1/acd$, 8
T^a , K	130	130
a , Å	17.493 (4)	18.293 (2)
c , Å	23.480 (8)	24.222 (9)
V , Å ³	7185 (3)	8105 (3)
ρ_{calc} , g cm ⁻³	4.82	5.40
μ (Mo $K\alpha$), cm ⁻¹	288.09	205.68
transm coeff range	0.08–0.11	0.16–0.18
$2\theta_{max}$	55	55
scan speed, °/min	14.65	3.97
Octants collected	hkl , $hk-l$, $h-k-l$, $h-kl$	hkl
No. data collected	15627	5064
No. unique data	2067	2334
No. obsd. reffs.	1390 [$F > 6\sigma(F)$]	2020 [$F > 4\sigma(F)$]
No. params. refined	61	61
R^b	4.02	3.71
R_w^b [$w = 1/\sigma^2(F_o)$]	4.26	4.37

^a Room temperature lattice dimensions (obtained from Guinier powder diffraction): $Sr_{14}AlSb_{11}$: $a = 17.542$ (6) Å, $c = 23.33$ (1) Å. $Ba_{14}AlSb_{11}$: $a = 18.360$ (8) Å, $c = 24.15$ (2) Å.

^b $R = \Sigma | |F_o| - |F_c| | / \Sigma |F_o|$ and $R_w = \Sigma | |F_o| - |F_c| | w^{1/2} / \Sigma |F_o w^{1/2}|$.

lected at 130 K on a Siemens R3m/v or a Syntex P2₁ diffractometer (Mo $K\alpha$, $\lambda = 0.71069$ Å, graphite monochromator). The unit cell parameters were obtained from least-squares refinement of 18 reflections with $25^\circ < 2\theta < 40^\circ$. The tetragonal I lattice was verified from axial photographs and systematic extinctions. No decomposition of the crystal was observed (inferred from the intensity of three check reflections). Crystallographic parameters are summarized in Table I. The data were corrected for Lorentz and polarization effects. Crystallographic programs were those of SHELXTL PLUS, Version 4.0, installed on a Micro VAX computer (14). Scattering factors and corrections for anomalous dispersion were from the "International Tables for X-Ray Crystallography" (15).

The structure of $Sr_{14}AlSb_{11}$ was refined by least-squares methods with the initial positions taken from $Ca_{14}AlSb_{11}$ (9). An absorption correction (16) was applied after the refinement converged with isotropic U 's. The U for Al was very small and, if Sb was put on that site, the U became very large. The lowest R , R_w were obtained if the U was fixed and the occupancy was allowed to refine. Since neither atom alone provided a satisfactory refinement, both Al and Sb were placed on that site. Their isotropic U 's were restricted to be equal and allowed to refine while their respective occupancies were refined so that the site was fully occupied. The refinement converged with the occupancy for Al 85% and that for Sb 15% on that site. All other atoms were refined using anisotropic U 's. A second data set was

taken on a crystal obtained from a different reaction and the results of the refinement were identical. In addition, similar results were obtained regardless of the absorption correction applied (XABS (16) or XEMP (14)).

The refinement for $\text{Ba}_{14}\text{AlSb}_{11}$ proceeded in a manner similar to that described above. The problems with the refinement of the isotropic U for Al were not nearly as severe as in the case of $\text{Sr}_{14}\text{AlSb}_{11}$. The Al/Sb refinement did not provide a significantly lower R value than the refinement with Al alone on that site; however, the isotropic U is more reasonable. The final occupancy was Al 96% and Sb 4% on that site. In addition, it was noted that the isotropic U for Sb(4) was about double the magnitude compared with other Sb atoms. This phenomenon has been noted in other isostructural compounds (12, 13). Although the origin of this disorder is not well understood, the large thermal parameter may be attributed to positional disorder. In extreme cases, it can be modeled by moving the atom off the 222 site (fully occupied) to the ..2 site (half occupied) (13). Axial photographs showed no indication of diffuse X-ray scattering or any other problems. The refinement with or without this disorder model gave similar R and R_w ; this paper gives the solution with the Sb(4) on the 222 site. An absorption correction was applied (16). All the atoms were refined with anisotropic U 's except the Al/Sb.

The largest features in the final difference map for the Sr and Ba analogs are $2.36 \text{ e}/\text{\AA}^3$, and $-5.71 \text{ e}/\text{\AA}^3$, respectively. Atomic coordinates and isotropic thermal parameters are given in Table II. The anisotropic thermal parameters are given in Table III, and the observed and calculated structure factor amplitudes are available as supplementary material.

Electrical characterization. Temperature-dependent resistivity was obtained for single crystals of $\text{Ca}_{14}\text{AlSb}_{11}$ and $\text{Sr}_{14}\text{AlSb}_{11}$. Care was taken to ensure that the crystals were not exposed to air. In a dry box

equipped with a microscope, a 2–3 mm long single crystal of the desired compound was placed on a piece of alumina (for support) and four Pt wires were attached to the crystal using silver epoxy. The crystal was transferred, under N_2 , to a furnace, and the epoxy was cured by heating to 100°C for 1 hr, under vacuum. After the epoxy was dry, the crystal was returned to the dry box and covered with a small amount of apeazon type-L grease to minimize exposure to air. The sample was then transferred to a sample holder and placed in a closed cycle refrigerator. A current of 1 mA (Keithley model 224 current source) was applied and the voltage was measured with a Keithley model 196 multimeter for $15 \text{ K} \leq T \leq 300 \text{ K}$ at 5 K intervals (17).

Temperature-dependent resistivity was measured on pressed pellets of $\text{Ba}_{14}\text{AlSb}_{11}$ because this compound decomposed too quickly to perform single-crystal studies. Temperature-dependent resistivity of a pressed pellet of $\text{Ca}_{14}\text{AlSb}_{11}$ was also obtained for comparison to the single crystal data. The samples were ground into powders and subsequently pressed into a 1 cm diameter by 2 mm thick pellet in a dry box. The pellet was then placed under four stainless steel probes with indium between each stainless steel probe and the pellet for better contact. This setup was then sealed under nitrogen and transferred to the closed cycle refrigerator. Resistivity measurements were taken using a procedure similar to that of the single-crystal setup. All samples exhibited ohmic behavior.

Results and Discussion

Structural results. Table IV gives selected bond distances and angles of the two new compounds, $A_{14}\text{AlSb}_{11}$, $A = \text{Sr}, \text{Ba}$, together with those for $\text{Ca}_{14}\text{AlSb}_{11}$ for comparison. Throughout the text the compounds are referred to by their ideal stoichiometry. The structure of the compounds, $A_{14}\text{AlSb}_{11}$ ($A = \text{Ca}, \text{Sr}, \text{Ba}$) can be described according to the Zintl concept as consisting of 14 A^{2+}

TABLE II
 ATOMIC COORDINATES ($\times 10^5$) AND ISOTROPIC EQUIVALENT THERMAL
 PARAMETERS ($\text{\AA}^2 \times 10^4$)

Atom	<i>x</i>	<i>y</i>	<i>z</i>	U^a
$Sr_{14}AlSb_{11}^b$				
Sb(1)	13346(5)	38346(5)	12500	111(3)
Sb(2)	338(5)	11375(6)	80981(5)	195(3)
Sb(3)	86930(5)	97506(5)	95280(4)	120(3)
Sb(4)	0	25000	12500	172(4)
Al(1)/Sb(5) ^{c,d}	0	25000	87500	78(16)
Sr(1)	17718(7)	29371(7)	57855(6)	124(4)
Sr(2)	97759(7)	12345(8)	548(6)	155(4)
Sr(3)	35527(10)	0	25000	104(5)
Sr(4)	81925(7)	9271(8)	84277(6)	138(4)
$Ba_{14}AlSb_{11}^e$				
Sb(1)	13025(4)	38025(4)	12500	119(2)
Sb(2)	243(4)	11897(4)	81537(3)	138(2)
Sb(3)	86731(3)	97499(4)	95343(3)	113(2)
Sb(4)	0	25000	12500	300(4)
Al(1)/Sb(5) ^{c,d}	0	25000	87500	79(17)
Ba(1)	17865(3)	29465(3)	57858(2)	129(2)
Ba(2)	97990(4)	12373(3)	64(3)	140(2)
Ba(3)	35659(5)	0	25000	124(2)
Ba(4)	81806(3)	9192(3)	84348(2)	138(2)

^a Equivalent isotropic U defined as one-third of the trace of the orthogonalized U_{ij} tensor.

^b $Sr_{14}Al_{0.85}Sb_{11.15}$.

^c $Sr_{14}AlSb_{11}$: Al(1) occ. = 0.211 (2) (85 %), Sb(5) occ. = 0.039 (2) (15 %). $Ba_{14}AlSb_{11}$: Al(1) occ. = 0.241 (2) (96 %), Sb(5) occ. = 0.009 (2) (4 %).

^d Refined isotropically.

^e $Ba_{14}Al_{0.96}Sb_{11.04}$.

cations, 4 Sb^{3-} anions, a $AlSb_4^{9-}$ tetrahedron, and a Sb_3^{7-} polyatomic anion. Although the charges given are formal charges, theoretical calculations indicate that this interpretation of the structure is correct (18). The structure has been described in detail previously (9). Briefly, the tetrahedra are stacked and translated by $\frac{1}{2}$ along the c axis, alternated by the polyatomic anions. The Sb_3^{7-} anions are staggered by 90° with respect to each other (along the c axis). The Sb^{3-} anions are located between the $AlSb_4^{9-}$ tetrahedra and the Sb_3^{7-} anions and form a spiral along a screw axis coincident with the c axis.

Figure 1 shows the $AlSb_4$ tetrahedron and the Sb_3 polyatomic unit with selected cations. The $AlSb_4^{9-}$ tetrahedra are distorted,

as they are in all compounds reported to date with the $Ca_{14}AlSb_{11}$ -structure type. Two other series of structures have been studied, the $A_{14}GaAs_{11}$ ($A = Ca, Sr$) (12, 13) and the $A_{14}MnBi_{11}$ ($A = Ca, Sr, Ba$) (6, 8, 10, 11) compounds. In both cases, there is a smooth increase in the metal–pnictide distance and the angle in the tetrahedra as a function of cation size. None of the published structures shows any sort of substitutional disorder in the $M-Pn$ tetrahedra. In the $A_{14}AlSb_{11}$ ($A = Sr, Ba$) series of compounds, there is apparently more electron density at the metal site in the tetrahedra than can be accounted for by one Al atom. Although it appears that this is less of a problem for the barium analogue, both structures exhibit this phenomenon. Ini-

TABLE III
 ANISOTROPIC DISPLACEMENT COEFFICIENTS ($\text{\AA}^2 \times 10^4$)

Atom	U_{11}	U_{22}	U_{33}	U_{23}	U_{13}	U_{12}
			$\text{Sr}_{14}\text{AlSb}_{11}^a$			
Sb(1)	111(4)	111(4)	111(7)	5(5)	1(3)	-1(3)
Sb(2)	109(5)	219(6)	257(6)	-17(4)	9(4)	123(4)
Sb(3)	159(5)	111(4)	90(5)	28(3)	19(3)	2(3)
Sb(4)	202(6)	202(6)	110(10)	114(8)	0	0
Sr(1)	133(6)	116(6)	124(7)	-1(5)	27(5)	-9(5)
Sr(2)	126(6)	139(6)	201(7)	17(5)	-19(5)	19(6)
Sr(3)	112(8)	117(8)	84(9)	0	0	14(7)
Sr(4)	114(6)	211(7)	88(6)	9(5)	14(5)	27(5)
			$\text{Ba}_{14}\text{AlSb}_{11}^b$			
Sb(1)	120(3)	120(3)	116(5)	3(3)	-6(2)	6(2)
Sb(2)	114(3)	137(3)	162(4)	-11(2)	7(3)	9(3)
Sb(3)	144(3)	103(3)	91(3)	20(2)	10(2)	-6(2)
Sb(4)	397(7)	397(7)	107(7)	302(8)	0	0
Ba(1)	139(3)	119(3)	128(3)	13(2)	0	-16(2)
Ba(2)	115(3)	134(3)	172(4)	16(2)	-9(2)	22(2)
Ba(3)	118(4)	130(4)	123(4)	0	0	9(3)
Ba(4)	109(3)	205(3)	101(3)	11(2)	10(2)	37(2)

Note. The anisotropic displacement exponent takes the form: $-2\pi^2(h^2a^*U_{11} + \dots + 2hka^*b^*U_{12})$.

^a $\text{Sr}_{14}\text{Al}_{0.85}\text{Sb}_{11.15}$.

^b $\text{Ba}_{14}\text{Al}_{0.96}\text{Sb}_{11.04}$.

tially it was thought that perhaps this problem resulted from inadequate absorption correction. Therefore, we collected a hemisphere of data on $\text{Sr}_{14}\text{AlSb}_{11}$ and performed the absorption correction with both XABS (16) and XEMP (14) programs, but the phenomenon persisted. Microprobe analyses of single crystals of $\text{Sr}_{14}\text{AlSb}_{11}$ confirm the nonstoichiometry, indicating less Al than expected. Since identical crystallographic results were obtained on two crystals from different reactions, it appears that this is an intrinsic phenomenon for $\text{Sr}_{14}\text{AlSb}_{11}$. In the report on the $\text{Ca}_{14}\text{AlSb}_{11}$ structure, no mention is made of any problems with occupancy, although the structure was refined with only the Sb U 's being anisotropic (9). Our microprobe data indicate that there may also be nonstoichiometry of the Al in $\text{Ca}_{14}\text{AlSb}_{11}$. The average stoichiometry from two crystals is $\text{Ca}_{13.9(2)}\text{Al}_{0.83(3)}\text{Sb}_{11.2(1)}$. There are no significant differences in lattice parameters obtained from this work compared

with the single crystal data (9), indicating that the small nonstoichiometry of the Al site cannot be confirmed based on powder X-ray data. Microprobe data could not confirm the nonstoichiometry of the $\text{Ba}_{14}\text{AlSb}_{11}$ sample. Interference of the Ba $L\alpha_2$ line with the Al $K\alpha_1$ line provided higher values for Al than expected and no excess in Sb is apparent. In this series of compounds, the Al-Sb distance, 2.718 Å (Ca), 2.833 Å (Sr), and 2.799 Å (Ba), does not increase smoothly with increasing size. This is attributed to the substitutional disorder on the Al site; with Sb substituting for the Al, longer distances are expected. Since this substitutional disorder is the greatest for the Sr analog, it may account for the slightly longer distance observed compared with the Ca and Ba compounds. Typical Al-Sb bond lengths in ternary Zintl compounds range from 2.674–2.816 Å (19–23). Typical bond lengths observed for Sb-Sb single bonds in solid state compounds are 2.84 Å in the Zintl

TABLE IV
 SELECTED BOND LENGTHS (Å) AND ANGLES (°)

	$\text{Ca}_{14}\text{AlSb}_{11}$ ^a	$\text{Sr}_{14}\text{AlSb}_{11}$ ^b	$\text{Ba}_{14}\text{AlSb}_{11}$ ^c
Sb(1)–Sb(4)	3.196(2)	3.302(2)	3.370(2)
Sb(1)–A(1) × 2	3.236(3)	3.373(2)	3.505(1)
Sb(1)–A(2) × 2	3.261(3)	3.415(2)	3.625(2)
Sb(1)–A(3) × 2	3.395(3)	3.579(1)	3.745(1)
Sb(1)–A(4) × 2	3.176(3)	3.363(2)	3.556(2)
Sb(2)–Al × 4	2.718(1)	2.833(1)	2.799(1)
Sb(2)–A(1)	3.237(3)	3.395(2)	3.601(2)
Sb(2)–A(1')	3.261(3)	3.427(2)	3.696(2)
Sb(2)–A(2)	3.161(3)	3.310(2)	3.4507(2)
Sb(2)–A(2')	3.742(3)	3.901(2)	3.968(2)
Sb(2)–A(3)	3.299(3)	3.471(2)	3.727(2)
Sb(2)–A(4)	3.182(3)	3.333(2)	3.476(2)
Sb(2)–A(4')	3.479(3)	3.681(2)	3.721(2)
Sb(3)–A(1)	3.202(3)	3.395(2)	3.492(2)
Sb(3)–A(1')	3.230(3)	3.357(2)	3.530(2)
Sb(3)–A(2)	3.163(3)	3.332(2)	3.509(2)
Sb(3)–A(2')	3.270(3)	3.443(2)	3.599(2)
Sb(3)–A(3)	3.133(3)	3.282(2)	3.417(2)
Sb(3)–A(4)	3.240(3)	3.409(2)	3.513(2)
Sb(3)–A(4')	3.271(3)	3.417(2)	3.533(2)
Sb(3)–A(4'')	3.744(3)	3.937(2)	4.069(2)
Sb(4)–A(1) × 4	3.211(3)	3.373(2)	3.551(1)
Sb(4)–A(2) × 4	3.429(3)	3.596(2)	3.814(2)
Sb(2)–Al–Sb(2')	107.3(1)	107.0(1)	105.4(1)
Sb(2)–Al–Sb(2'')	114.0(1)	114.6(1)	117.9(1)

^a Reference (9).^b $\text{Sr}_{14}\text{Al}_{0.85}\text{Sb}_{11.15}$.^c $\text{Ba}_{14}\text{Al}_{0.96}\text{Sb}_{11.04}$.

compound, $\text{Ca}_{11}\text{InSb}_9$ (24), to 2.908 Å in elemental Sb (25). Substitutional disorder has not been observed in any of the other $A_{14}\text{MPn}_{11}$ compounds prepared to date (6, 8, 10–13, 26). Perhaps the reason substitutional disorder is observed in these compounds is that the size of the Al^{3+} ion is too small to comfortably accommodate the AlSb_4 tetrahedron. Since these reactions are prepared from stoichiometric amounts of the elements in Nb tubes, it is also possible that some of the Al alloys with the Nb, giving rise to an Al-deficient sample. It should be noted, however, that no Nb was detected in any of the crystals by microprobe. In addition, reactions run with excess Al to pro-

duce $\text{Sr}_{14}\text{AlSb}_{11}$ gave identical lattice parameters compared to $\text{Sr}_{14}\text{AlSb}_{11}$ prepared from stoichiometric amounts of the elements. The angles of the tetrahedron in $\text{Sr}_{14}\text{AlSb}_{11}$ (107.0° and 114.6°) are almost identical to the Ca analog (107.3° and 114.6°). Based on the $A_{14}\text{GaAs}_{11}$ ($A = \text{Ca}, \text{Sr}$) (12, 13) and the $A_{14}\text{MnBi}_{11}$ ($A = \text{Ca}, \text{Sr}, \text{Ba}$) (8) series of compounds, we expect the tetrahedral distortion to increase slightly (about 1°) as a function of alkaline earth cation size. The Ba analog is distorted (105.4° and 117.9°) compared with the Sr and the Ca analogs. The absence of a linear dependence of the tetrahedral angle with the size of the cation in this series of compounds is probably due

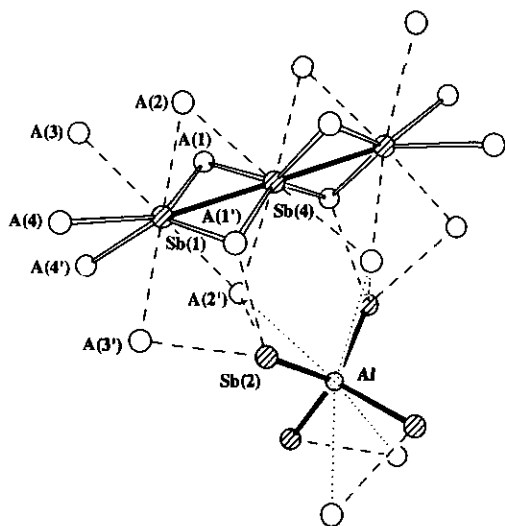


FIG. 1. A perspective view showing the relative orientation of the AISb_4 tetrahedron and Sb_3 unit with selected cations.

to more subtle influences than simple steric effects.

The Sb–Sb bond distance in the Sb_3 unit increases as a function of increasing cation size, 3.196 Å (Ca), 3.302 Å (Sr), and 3.370 Å (Ba). For the compounds, $\text{A}_{14}\text{GaAs}_{11}$ ($\text{A} = \text{Ca}, \text{Sr}$), the central As is elongated along the bond (Ca) or modeled with two central As sites that are both half occupied

(Sr) (13). A similar phenomenon is observed for $\text{Ba}_{14}\text{AlSb}_{11}$; the equivalent isotropic U for the central Sb, Sb(4), is two times larger than the other Sb atoms in the structure. The anisotropic U_{11} and U_{22} are large compared with U_{33} . This is attributed to positional disorder along the Sb–Sb bond that makes the two Sb–Sb distances in this polyatomic unit inequivalent. The distances in this Sb_3^{7-} unit are larger than a normal Sb–Sb single bond, but the increased distance compared with the single bond is consistent with those observed in other three-center four-electron hypervalent ions (27). Theoretical calculations (18) on $\text{Ca}_{14}\text{GaAs}_{11}$ are in agreement with this interpretation of the three atom polyatomic unit.

The Sb^{3-} anions are located between the tetrahedra and the Sb_3^{7-} unit and form a spiral along c . These anions are not considered to be part of a homoatomic unit. The shortest distances to other Sb are those within the spiral, 4.336 Å and 4.726 Å (Sr), and 4.488 Å and 4.849 Å (Ba). The shorter distance (4.336 Å (Sr) and 4.488 Å (Ba)) is too long to be considered a bonding interaction, but these atoms may be considered as loosely associated $\text{Sb}\cdots\text{Sb}$ dimers. Figure 2 shows the coordination of the Sb^{3-} with the cations and the relative orientation of these units with respect to the tetrahedron and the Sb_3^{7-} polyatomic unit.

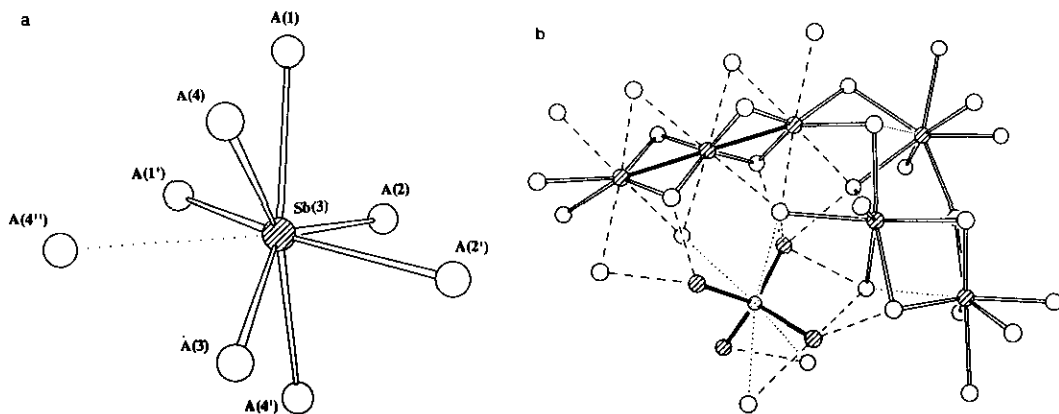


FIG. 2. (a) A view of Sb(3) showing the local coordination and (b) showing the relative orientation of the Sb(3) with respect to the AISb_4 tetrahedron and the Sb_3 unit.

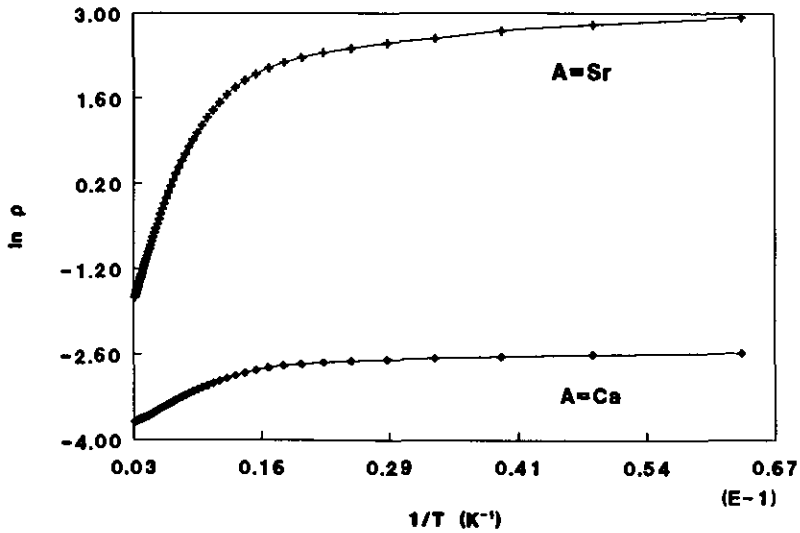


FIG. 3. $\ln \rho$ versus $1/T$ (K^{-1}) ($T = 10$ – 300 K) of single crystals of $A_{14}AlSb_{11}$ ($A = Sr, Ca$).

Resistivity. Figure 3 shows the $\ln \rho$ vs $1/T$ data for $Ca_{14}AlSb_{11}$ and $Sr_{14}AlSb_{11}$. The Ca and Sr samples were single crystals and the room temperature resistivities are small, $2.3 \times 10^{-2} \Omega \text{ cm}$ (Ca) and $5.9 \times 10^{-1} \Omega \text{ cm}$ (Sr). Data were collected over the entire temperature range, 300–15 K. The data show saturation effects at low temperature,

typical of semiconductors. The data for $Ba_{14}AlSb_{11}$ were taken on a pressed pellet. The crystals of $Ba_{14}AlSb_{11}$ are significantly more air sensitive than either the Ca or Sr analogs and decompose upon annealing the silver epoxy. The resistance of the Ba pressed pellet becomes too large to measure at low temperatures so the data were only

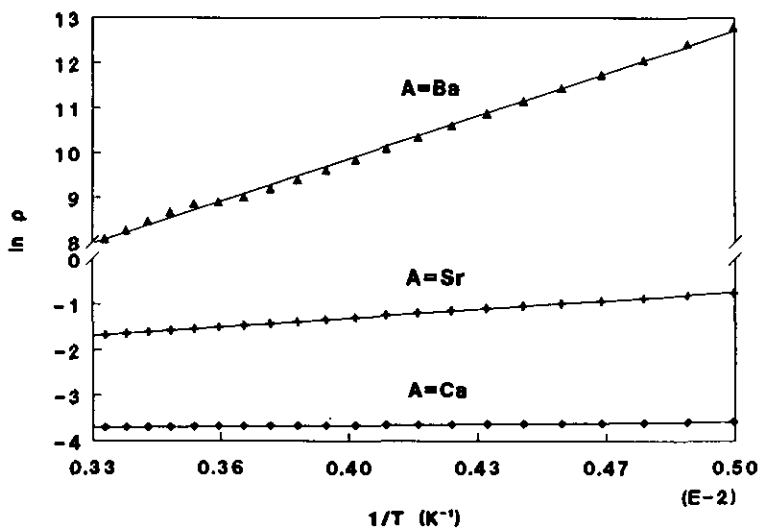


FIG. 4. $\ln \rho$ versus $1/T$ (K^{-1}) ($T = 200$ – 300 K) of single crystals of $A_{14}AlSb_{11}$ ($A = Sr, Ca$) and of a pressed pellet of $Ba_{14}AlSb_{11}$. The lines show the least-squares fit to the data.

TABLE V
RESISTIVITY DATA FOR $A_{14}\text{AlSb}_{11}$ ^a

A	Temp. (K)	E_a (eV)	ρ_{300} ($\Omega\text{-cm}$)	ρ_0 ($\Omega\text{-cm}$)
Ca ^b	100–300	0.014	2.3×10^{-2}	4.0
Ca ^c	100–300	0.014	2.6×10^2	2.2
Sr ^b	150–300	0.067	5.9×10^{-1}	1.9
Ba ^c	200–300	0.48	3.2×10^3	1.3

^a Values obtained from the equation: $\ln \rho = (E_a/2k_b T) - \rho_0$.

^b Single crystal.

^c Pressed pellet.

taken from 300–185 K. Figure 4 shows the $\ln \rho$ vs $1/T$ data from 300–200 K with least-squares fits for all three compounds. Activation energies and room-temperature resistivities are given in Table V. In order to compare data from a pressed pellet with that from a single crystal, data were also obtained for a pressed pellet of $\text{Ca}_{14}\text{AlSb}_{11}$. The data yielded a similar value for the activation energy regardless of whether the sample was a crystal or a pressed pellet. The room-temperature resistivity for the pressed pellet was $2.6 \times 10^2 \Omega \text{ cm}$, about four orders of magnitude higher than the single crystal value. This may be attributed to anisotropy effects as well as to intergranular boundary effects. The room temperature resistivity for the $\text{Ba}_{14}\text{AlSb}_{11}$ pressed pellet is an order of magnitude larger than the $\text{Ca}_{14}\text{AlSb}_{11}$ pressed pellet. In addition, the activation energy for $\text{Ba}_{14}\text{AlSb}_{11}$ is an order of magnitude larger than the activation energies for either the Sr or Ca analogues. This may be attributed to the large amount of substitutional disorder observed in the Sr and Ca analogues. If these compounds could be prepared without substitutional disorder on the Al site, one might expect the resistivities and bandgaps to be higher. The activation energies could not be confirmed as band gaps from room temperature optical, near IR, IR, or far IR data. The samples are opaque in the wavelength regions studied, indicating that these compounds are probably narrow gap semiconductors. The

$\text{A}_{14}\text{AlSb}_{11}$ series of compounds shows increasing band gap with electron donor ability. This is also observed for the $\text{A}_{14}\text{MnBi}_{11}$ compounds, with $A = \text{Ca}, \text{Sr}$ being metals with low resistance and the $A = \text{Ba}$ samples having higher resistance (8).

Acknowledgments

We thank Professors David J. Webb and Håkon Hope for useful discussion, Professor Anne Hofmeister for far-IR and IR data and Dianna Young for assistance with the preliminary aspects of this project. The research was funded by National Science Foundation Grants DMR-8913831 and DMR-9201041.

References

1. H. SCHÄFER, B. EISENMANN, AND W. MÜLLER, *Angew. Chem. Int. Ed. Engl.* **12**, 694 (1973).
2. H. SCHÄFER, *Annu. Rev. Mater. Sci.* **15**, 1 (1985).
3. R. NESPER, *Prog. Solid State Chem.* **20**, 1 (1990).
4. B. EISENMANN AND H. SCHÄFER, *Rev. Inorg. Chem.* **3**, 29 (1981).
5. E. ZINTL, *Angew. Chem.* **52**, 1 (1939).
6. S. M. KAUZLARICH, T. Y. KUROMOTO, AND M. M. OLMSTEAD, *J. Am. Chem. Soc.* **111**, 8041 (1989).
7. S. M. KAUZLARICH, *Comments Inorg. Chem.* **10**, 75 (1990).
8. T. Y. KUROMOTO, S. M. KAUZLARICH, AND D. J. WEBB, *Chem. Mater.* **4**, 435 (1992).
9. G. CORDIER, H. SCHÄFER, AND M. STELTER, *Z. Anorg. Allg. Chem.* **519**, 183 (1984).
10. T. Y. KUROMOTO, S. M. KAUZLARICH, AND D. J. WEBB, *Mol. Cryst. Liq. Cryst.* **181**, 349 (1990).
11. D. J. WEBB, T. Y. KUROMOTO, AND S. M. KAUZLARICH, *J. Magn. Magn. Mater.* **98**, 71 (1991).
12. S. M. KAUZLARICH, M. M. THOMAS, D. A. ODINK, AND M. M. OLMSTEAD, *J. Am. Chem. Soc.* **113**, 7205 (1991).
13. S. M. KAUZLARICH AND T. Y. KUROMOTO, *Croat. Chim. Acta* **64**, 343 (1991).
14. G. M. SHELDRICK, "SHELXTL PLUS, A Program for Crystal Structure Determination," Version 4.2, Siemens Analytical X-ray Instruments, Madison, WI (1990).
15. Scattering factors (neutral atoms) are from "International Tables for X-ray Crystallography," Vol. C, Reidel, Boston (1992).
16. Program XABS provides an empirical correction based on Fo and Fc differences. H. HOPE AND B. MOEZZI, "XABS," Chemistry Department, University of California, Davis (1987).
17. J. E. SUNSTROM IV, "DCRES, A Quickbasic Program for Temperature Dependent Resistivity Data Collection and Statistical Analysis," unpublished, University of California, Davis (1991).

18. R. F. GALLUP, C. Y. FONG, AND S. M. KAUZLARICH, *Inorg. Chem.* **31**, 115 (1992).
19. G. CORDIER, E. CZECH., M. JAKOWSKI, AND H. SCHÄFER, *Rev. Chim. Miner.* **18**, 9 (1981).
20. G. CORDIER, G. SAVELSBERG, AND H. SCHÄFER, *Z. Naturforsch. B* **37**, 975 (1982).
21. G. CORDIER, M. STELTER, AND H. SCHÄFER, *J. Less-Common Met.* **98**, 285 (1984).
22. G. CORDIER, H. SCHÄFER, AND M. STELTER, *Z. Naturforsch. B* **39**, 727 (1984).
23. G. CORDIER AND M. STELTER, *Z. Naturforsch. B* **43**, 463 (1988).
24. G. CORDIER, H. SCHÄFER, AND M. STELTER, *Z. Naturforsch. B* **40**, 868 (1985).
25. A. F. WELLS, "Structural Inorganic Chemistry," Oxford Univ. Press, Oxford, UK, (1984).
26. A. REHR, T. Y. KUROMOTO, S. M. KAUZLARICH, J. DEL CASTILLO AND D. J. WEBB, submitted for publication.
27. A. J. ARDUENGO III AND D. A. DIXON, in "Heteroatom Chemistry" (E. Block, Ed.), VCH Publishers, New York (1990).